

Supplementary Figures

Kinetic characterization of the immune response to methicillin-resistant *Staphylococcus aureus* subcutaneous skin infection

Miranda J. Ridder¹, Aubrey K. Gilchrist¹, Hongyan Dai³, Michele T. Pritchard², Mary A. Markiewicz^{1#}, Jeffrey L. Bose^{1#}

¹Department of Microbiology, Molecular Genetics & Immunology, University of Kansas Medical Center, Kansas City, Kansas

²Department of Pharmacology, Toxicology and Therapeutics, University of Kansas Medical Center, Kansas City, Kansas

³Department of Pathology and Laboratory Medicine, University of Kansas Medical Center, Kansas City, Kansas

#Address correspondence to Jeffrey L. Bose, jbose@kumc.edu and Mary A. Markiewicz, mmarkiewicz@kumc.edu

Figure S1. Magnified histology images at 8 hours p.i.

Figure S2. Magnified histology images at 1 d.p.i.

Figure S3: Magnified histology images at 3 d.p.i.

Figure S4: Magnified histology images at 5 d.p.i.

Figure S5. Magnified histology images at 7 d.p.i.

Figure S6. Magnified histology images at 9 d.p.i.

Figure S7. Magnified histology images at 11 d.p.i.

Figure S8. Magnified histology images at 13 d.p.i.

Figure S9. Magnified histology images at 15 d.p.i.

Figure S10. IL-1 α levels in heathy and infected skin.

Figure S11. Defined APC populations.

Figure S12. Additional APC populations.

Figure S13. B cell dynamics at the site of infection.

Figure S14. Gating strategy for antibody Panel 1.

Figure S15. Gating strategy for antibody Panel 2.

Figure S16. Gating strategy for antibody Panel 3.

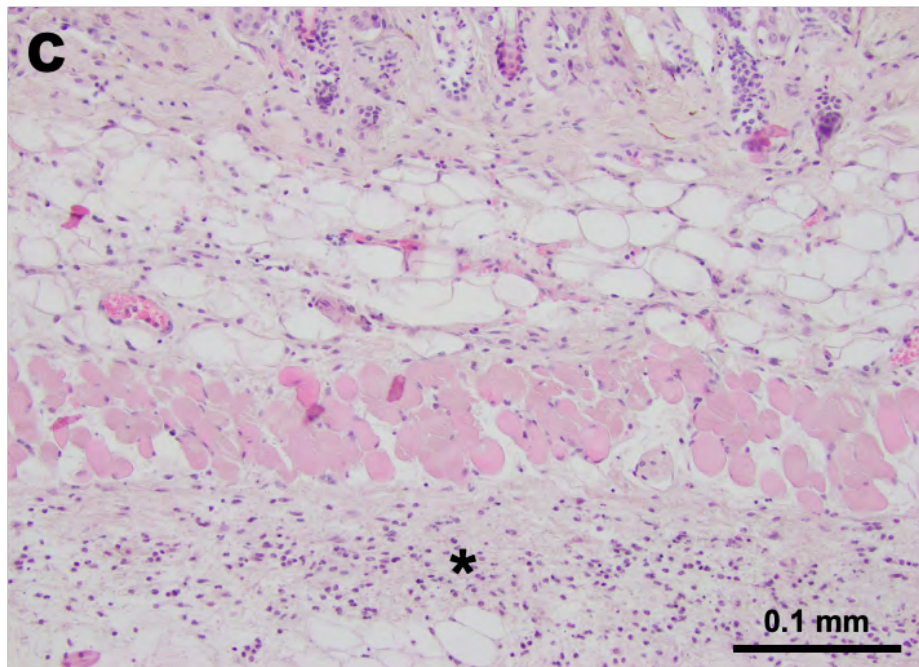
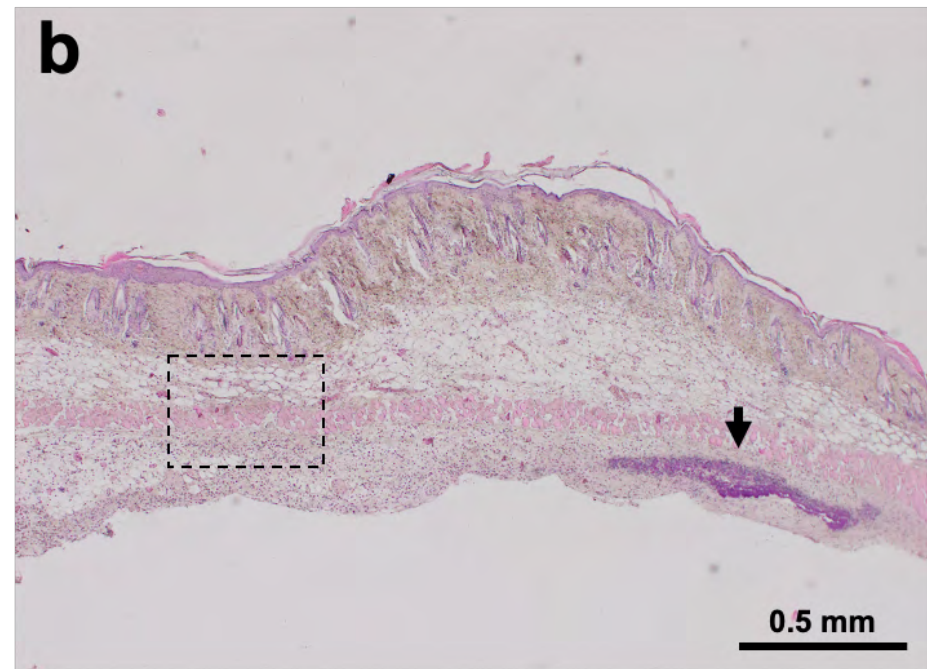
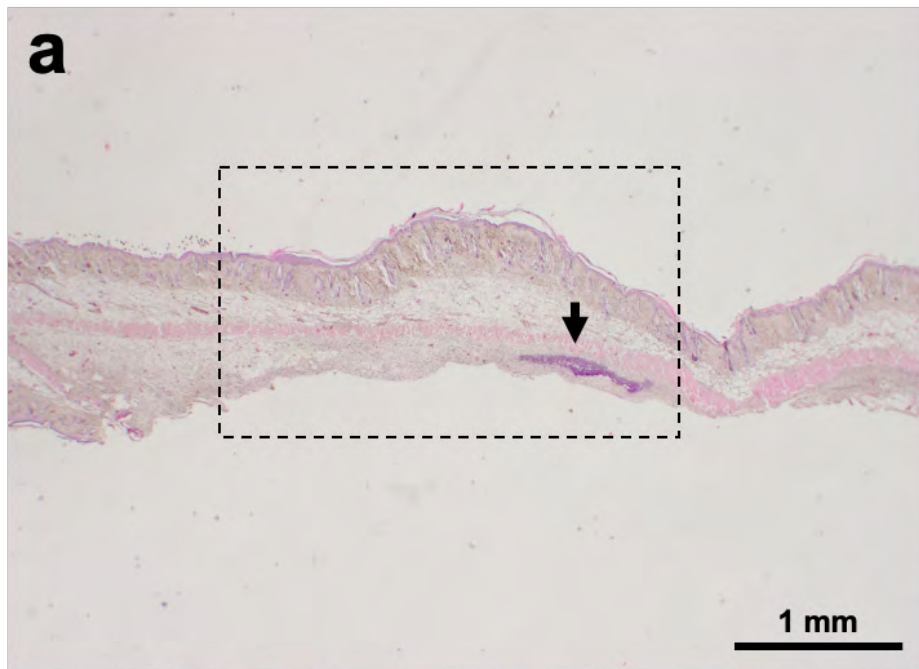


Figure S1. Histopathology 8h post infection. Panels are (a) 20X, (b) 40X, and (c) 200X. Box in panel a indicates area viewed in panel b. Similarly, the box in panel a indicates field of view of panel c. Bacteria (arrow, a-b) can be identified in the soft tissue below a thin layer of skeletal muscle. Mild inflammatory changes characterized by sparse neutrophilic infiltrate (asterisk, c) is present. Significant tissue necrosis is not appreciated. Scale bars are as indicated.

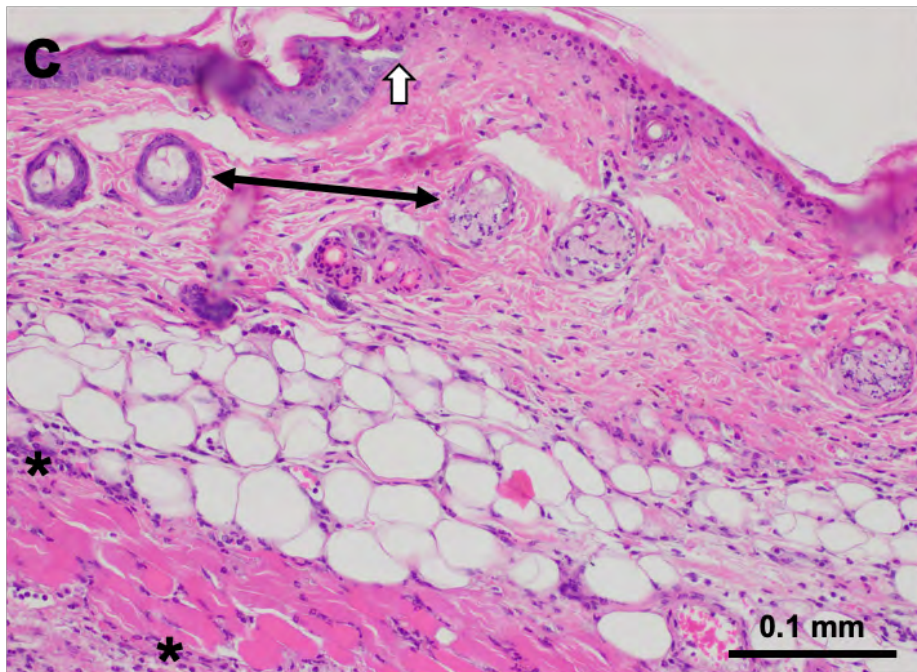
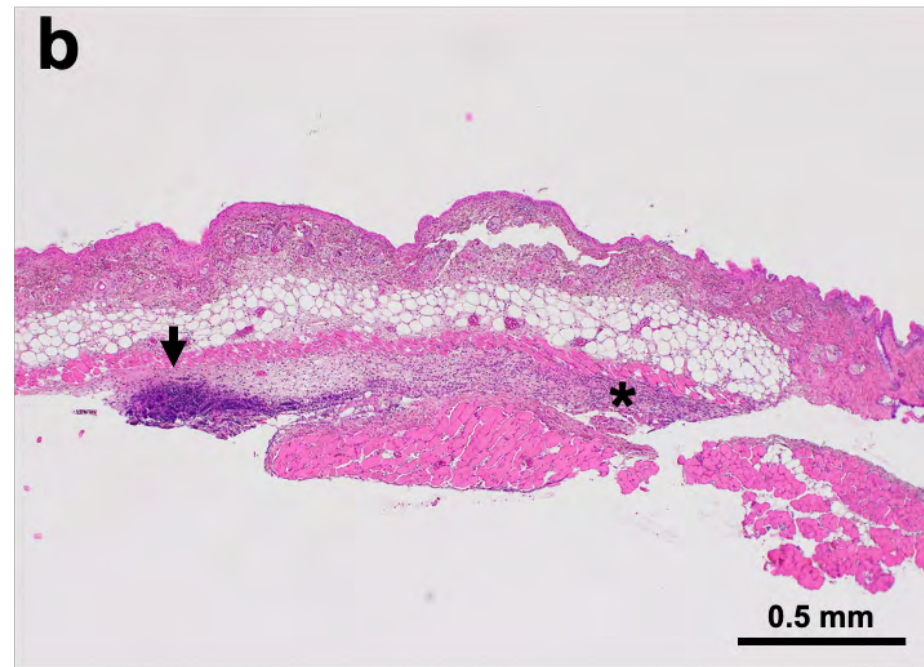
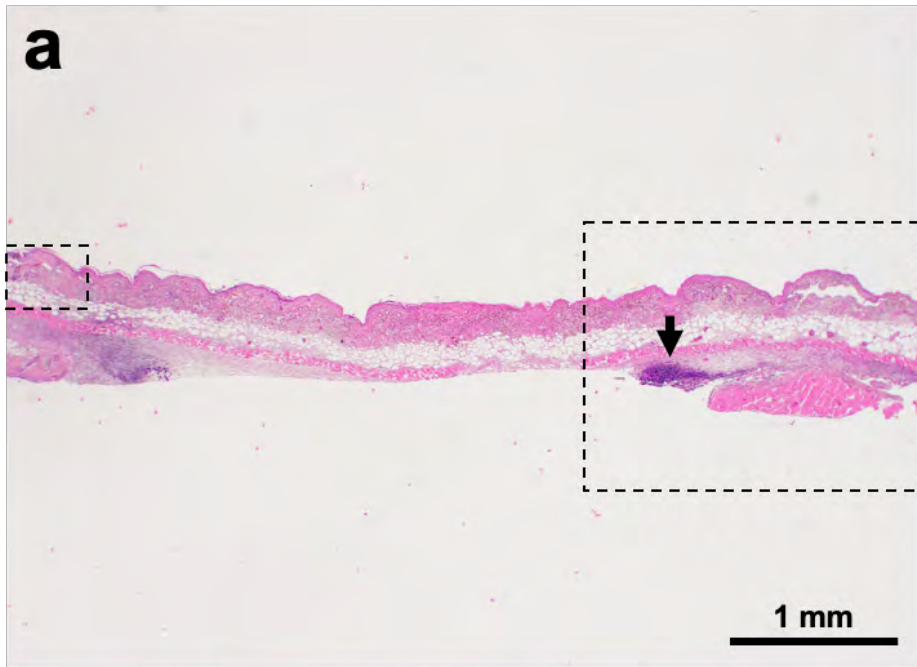


Figure S2. Histopathology 1 day post infection. Panels are (a) 20X, (b) 40X, and (c) 200X. Large box and small box in panel a indicate areas viewed in panels b and c, respectively. Larger bacterial nests (arrow, a-b) and denser, neutrophil-rich inflammatory infiltrate (asterisk, b-c) are appreciated at this time point relative to 8h post infection (Figure S1.). Early signs of tissue damage characterized by subtle nuclear dissolution can be observed (c, left side of the double arrow indicates a normal skin adnexal structure in contrast to a disintegrating one on the right; empty arrow indicates the dividing point between normal and abnormal epidermis). Scale bars are as indicated.

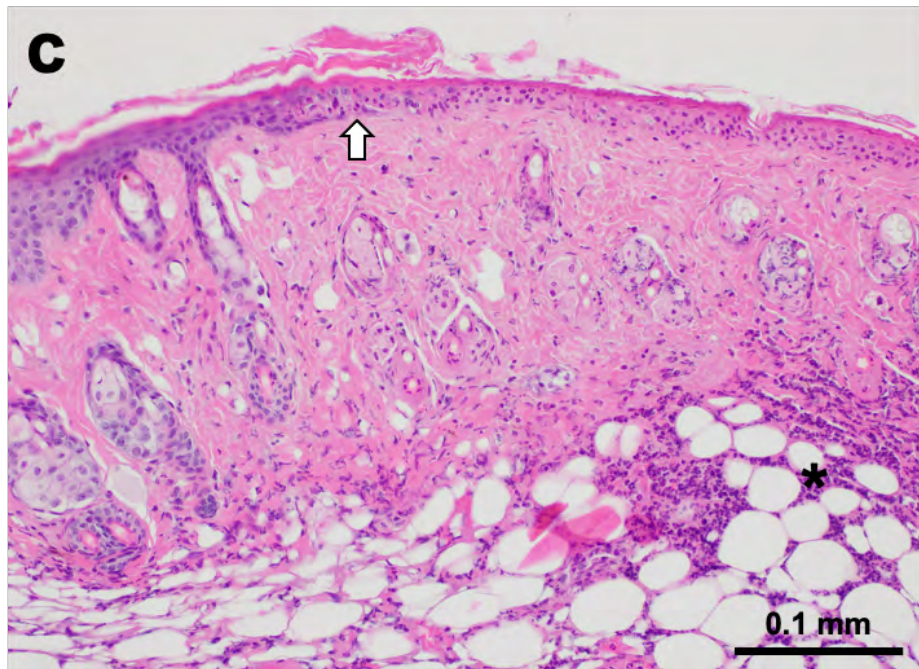
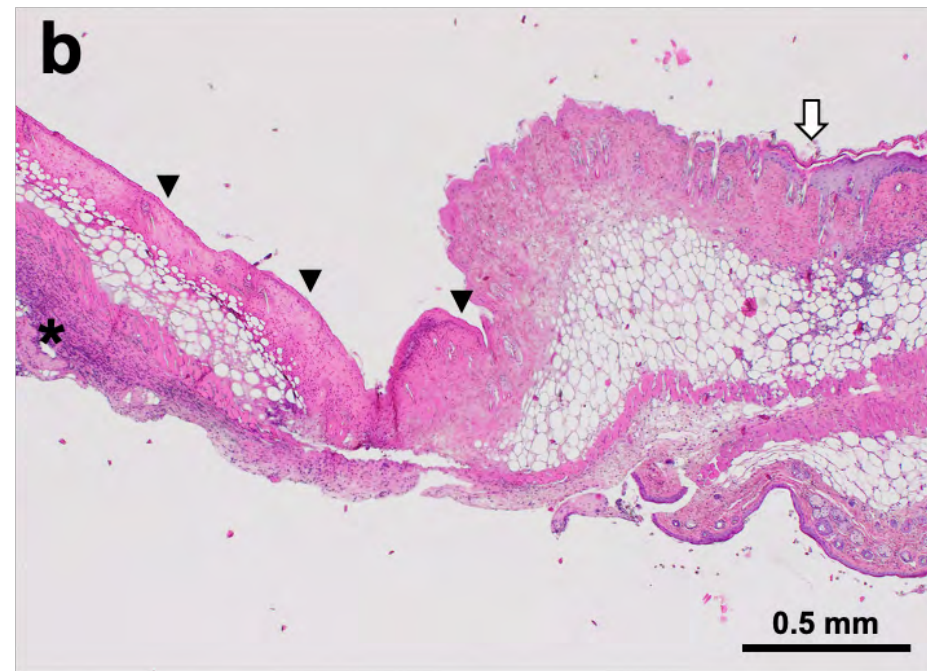
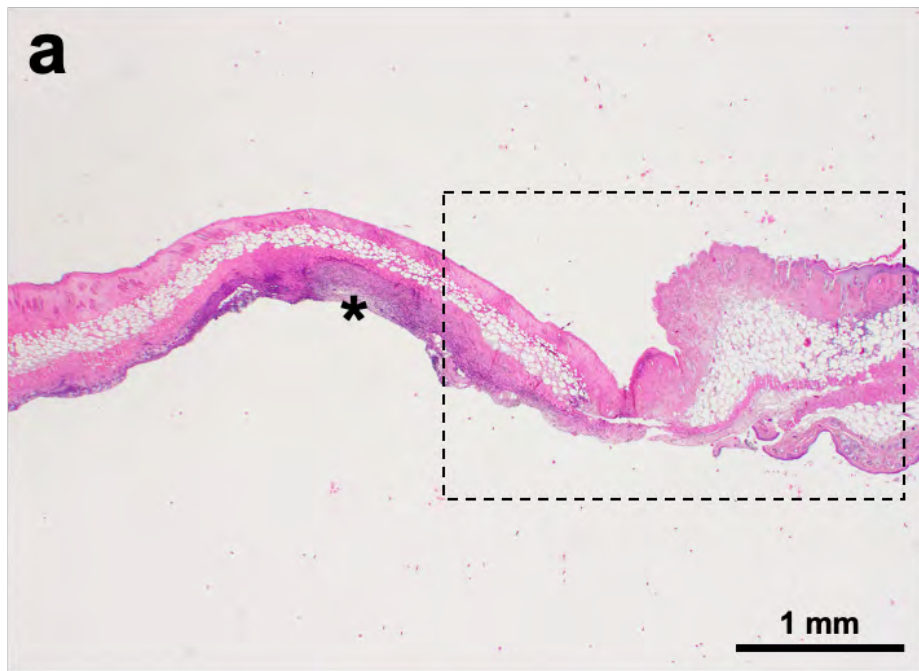


Figure S3. Histopathology 3 days post infection. Panels are (a) 20X, (b) 40X, and (c) 200X. Box in panel a indicates area viewed in panel b. Panel c is taken from outside the view in panel a. Prominent inflammation is present (asterisk, a-c). Significant tissue necrosis involving skin and subcutaneous tissue with tissue collapse is present (arrowhead, b). The dividing point between normal and abnormal tissue is depicted in panel c (empty arrow). Scale bars are as indicated.

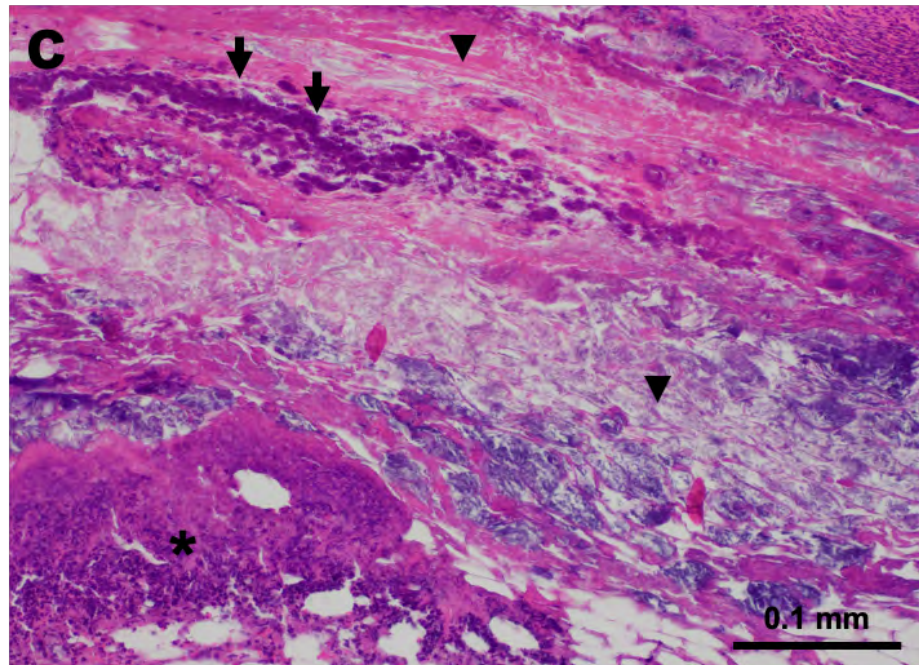
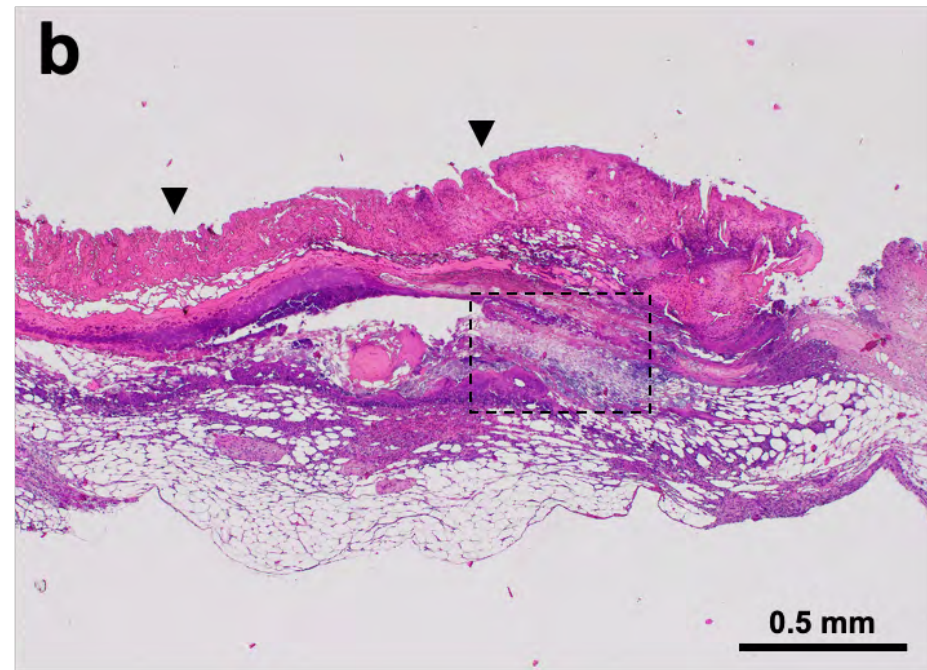
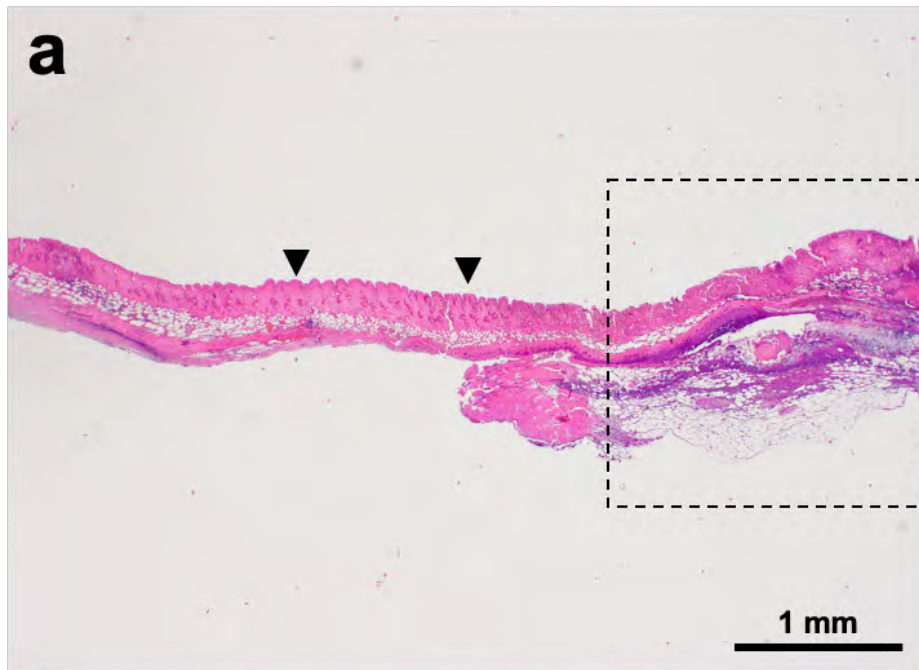


Figure S4. Histopathology 5 days post infection. Panels are (a) 20X, (b) 40X, and (c) 200X. Box in panel a indicates area viewed in panel b. Similarly, the box in panel b indicates field of view of panel c. There is prominent tissue necrosis (arrowhead, a-b). Bacteria (arrow, c) and inflammatory infiltrate (asterisk, c) are intermixed with necrotic debris (arrowhead, c). Scale bars are as indicated.

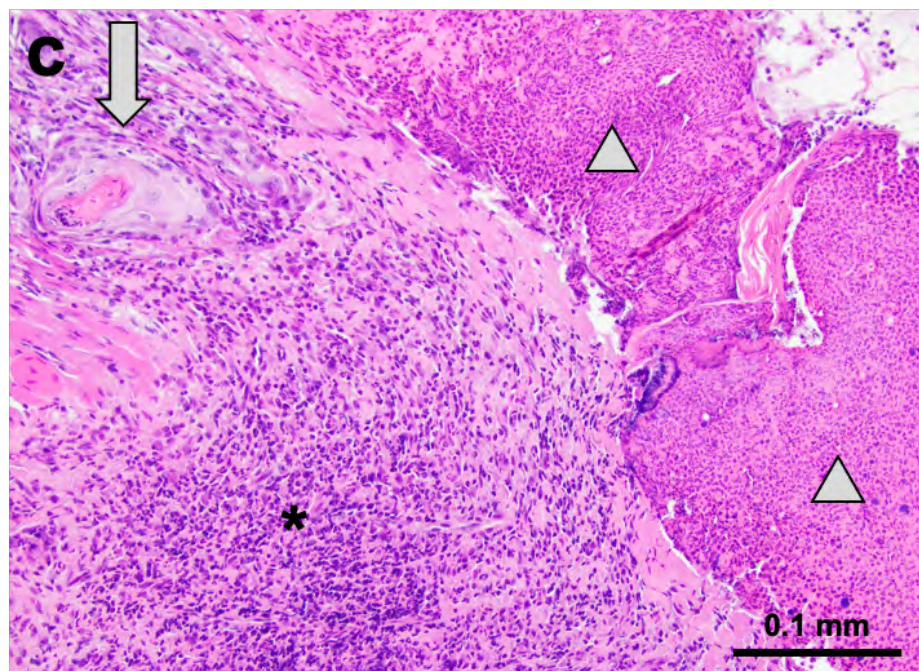
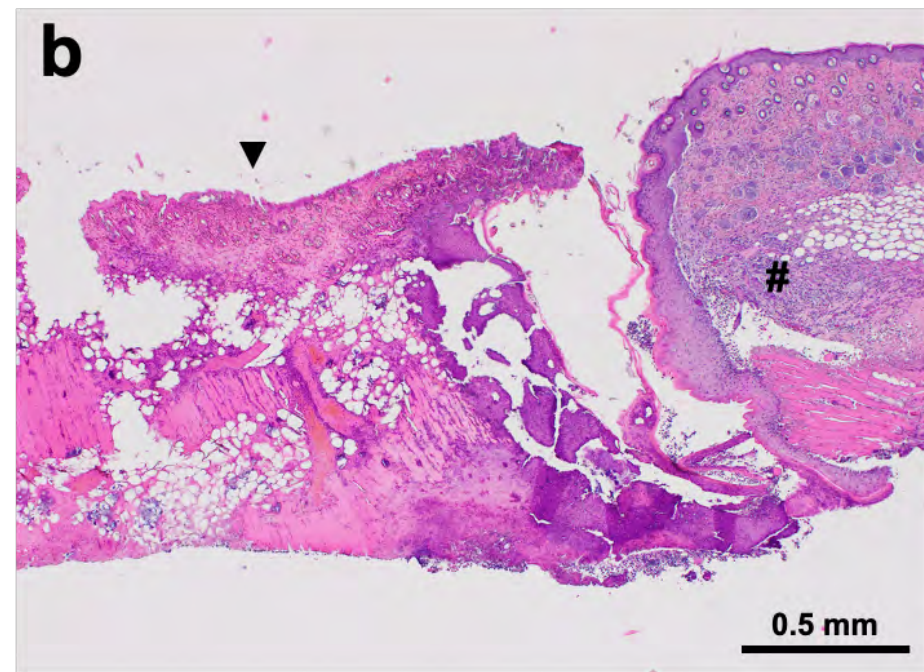
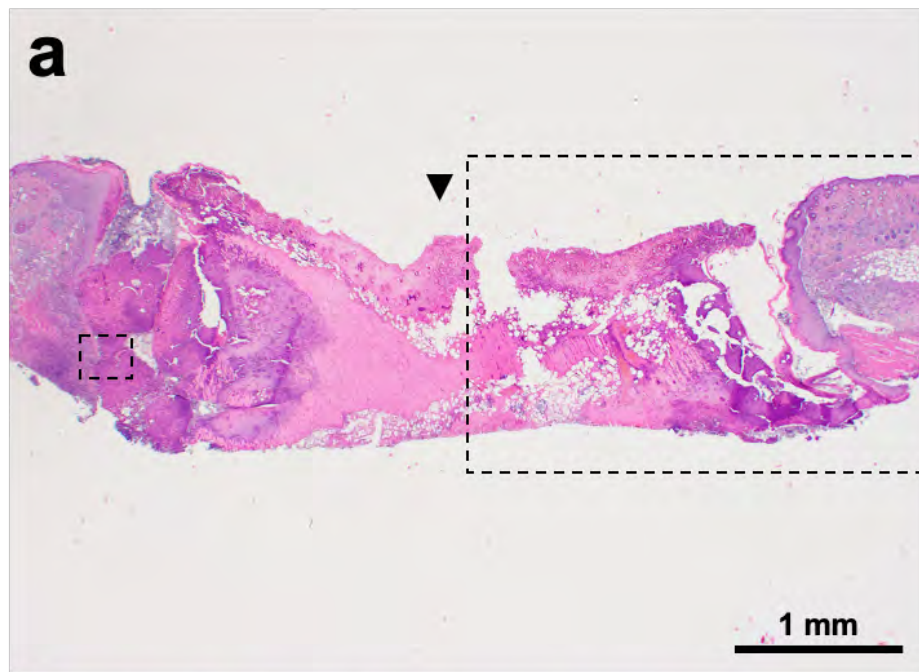


Figure S5. Histopathology 7 days post infection. Panels are (a) 20X, (b) 40X, and (c) 200X. Large box and small box in panel a indicate areas viewed in panels b and c, respectively. Full thickness tissue necrosis involving the epidermis, dermis, adipose tissue, and skeletal muscle has led to the formation of a discrete ulcer (arrowhead, a-b). The viable tissue flanking the lesion shows early granulation tissue formation (#, b). (c) Dense mixed inflammation (asterisk) lateral to necroinflammatory debris (grey triangles). Grey arrow highlights reactive epidermis. Scale bars are as indicated.

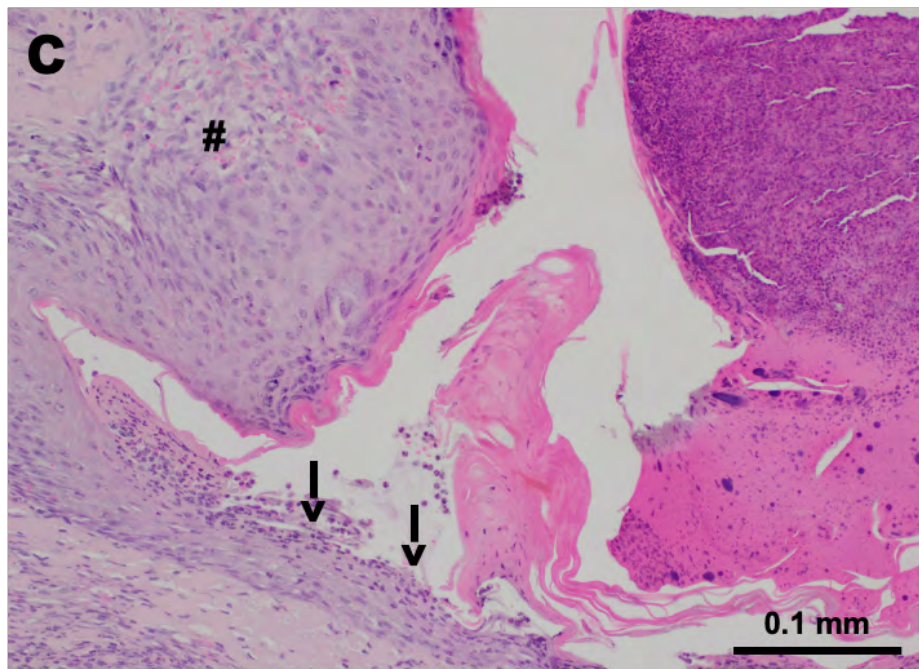
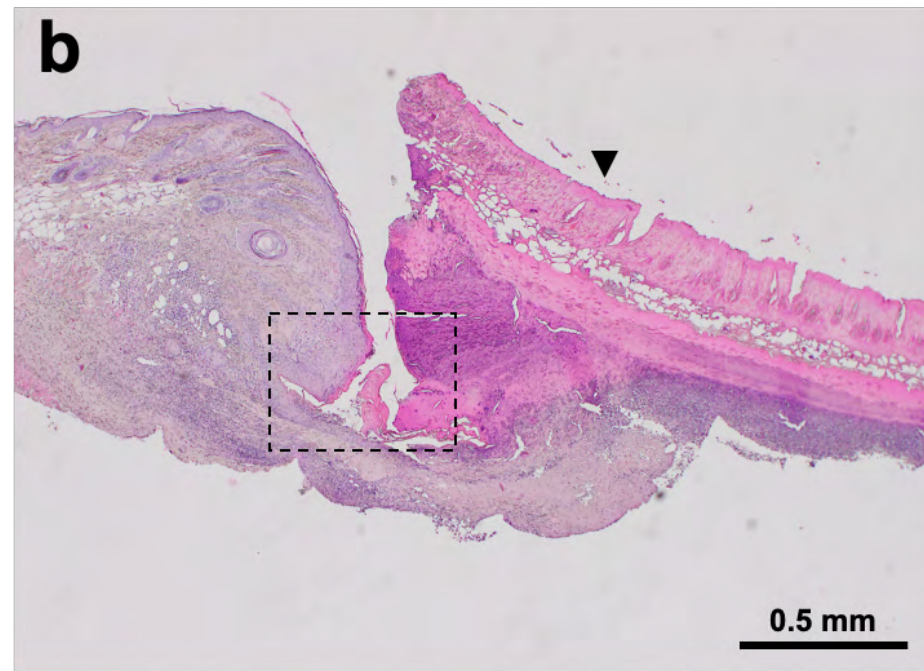
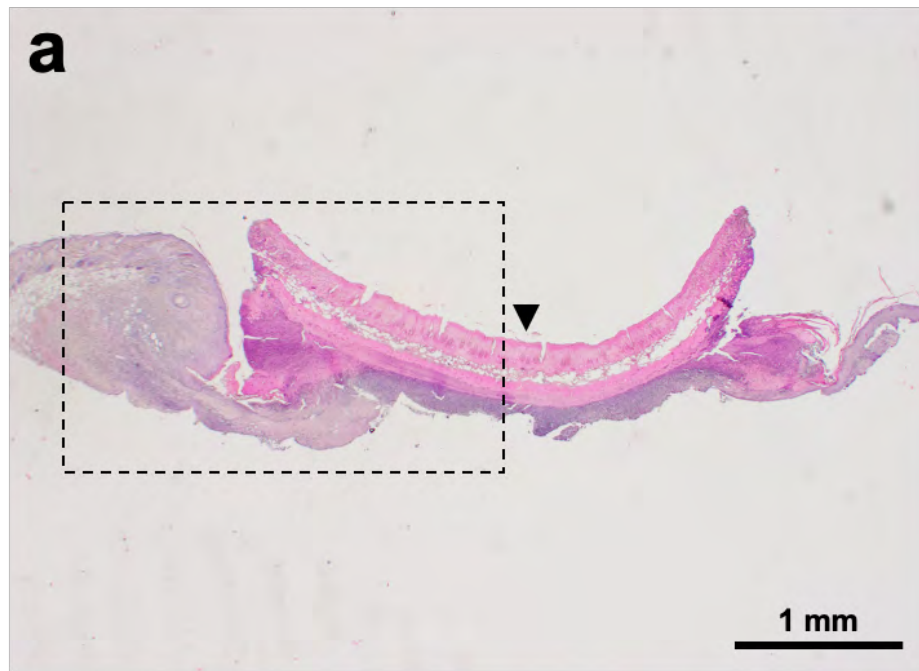


Figure S6. Histopathology 9 days post infection. Panels are (a) 20X, (b) 40X, and (c) 200X. Box in panel a indicates area viewed in panel b. Similarly, the box in panel b indicates field of view of panel c. Reparative changes are evident. a) central ulcer covered with scab (arrowhead, a-b) is flanked by reactive epidermis, granulation tissue (#, c), and early re-epithelialization (empty head arrow, c). Scale bars are as indicated.

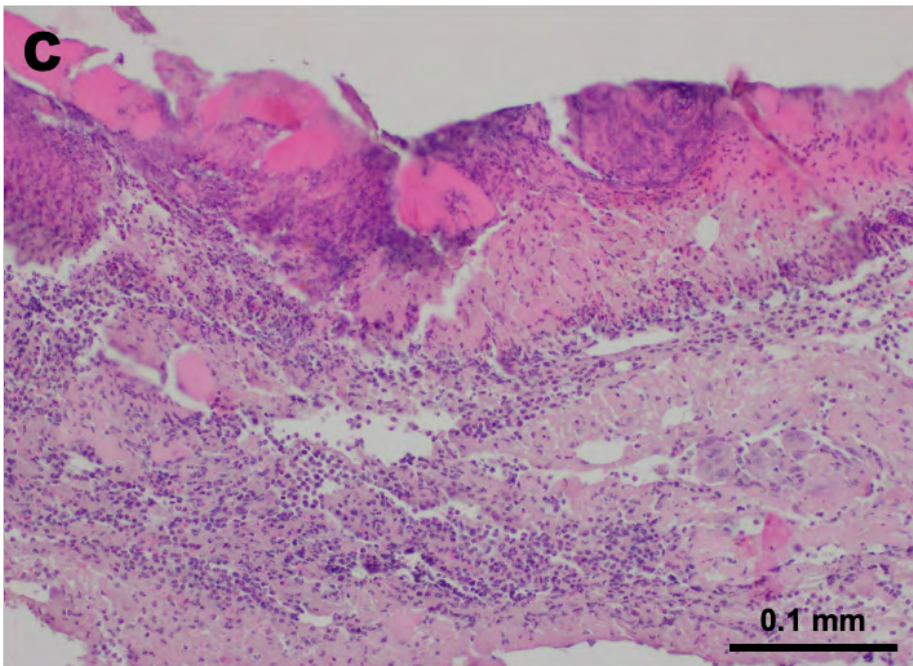
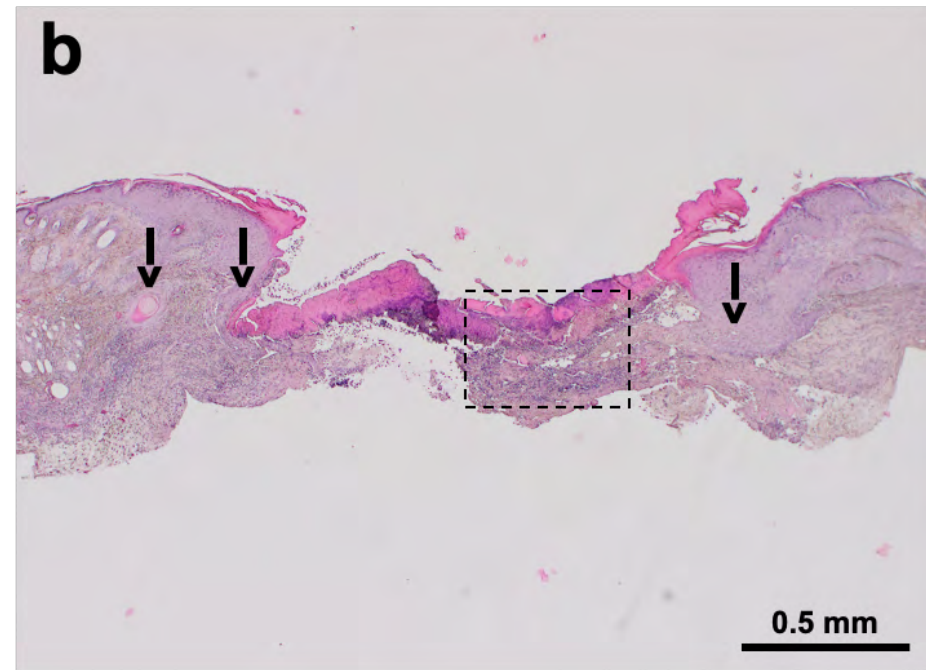
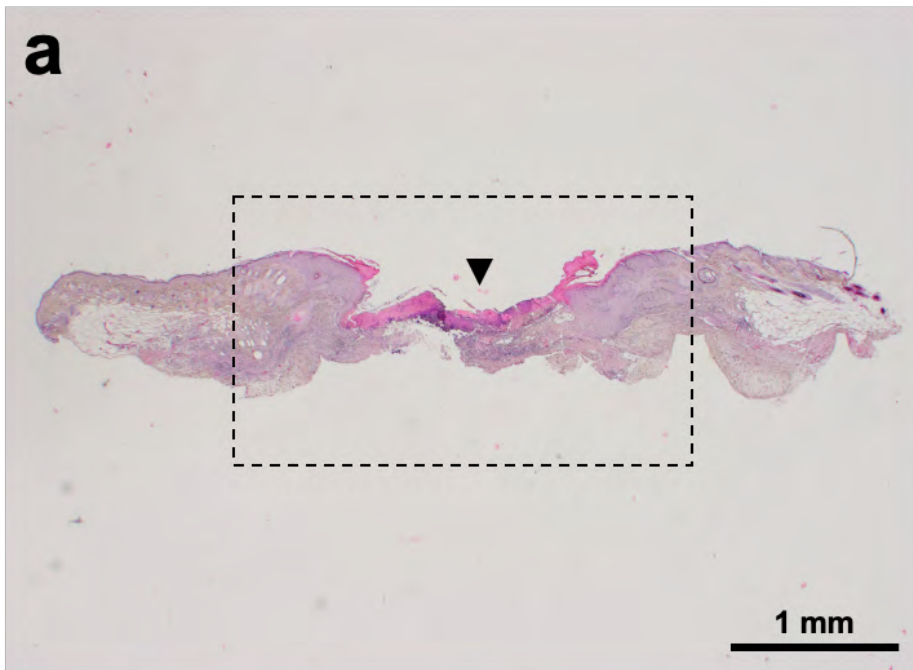


Figure S7. Histopathology 11 days post infection. Panels are (a) 20X, (b) 40X, and (c) 200X. Box in panel a indicates area viewed in panel b. Similarly, the box in panel b indicates field of view of panel c. The wound is smaller in size at this time point relative to 9 days post infection (Figure S6) (arrowhead, a). The epidermis is proliferative and thickened indicating re-epithelialization at the wound edges (empty head arrows, b). Higher power view demonstrates persistent central necroinflammatory tissue (c). Scale bars are as indicated.

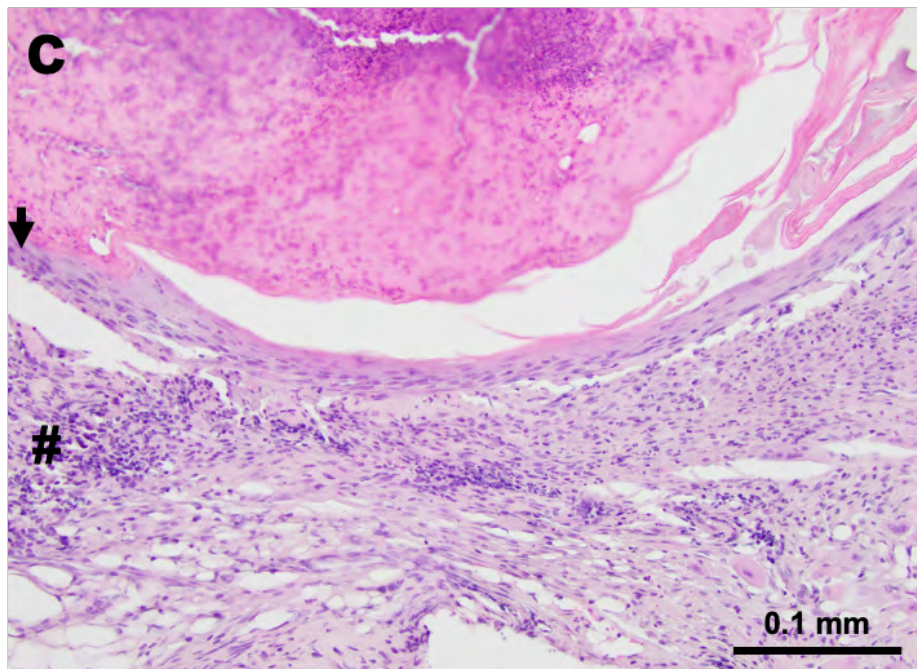
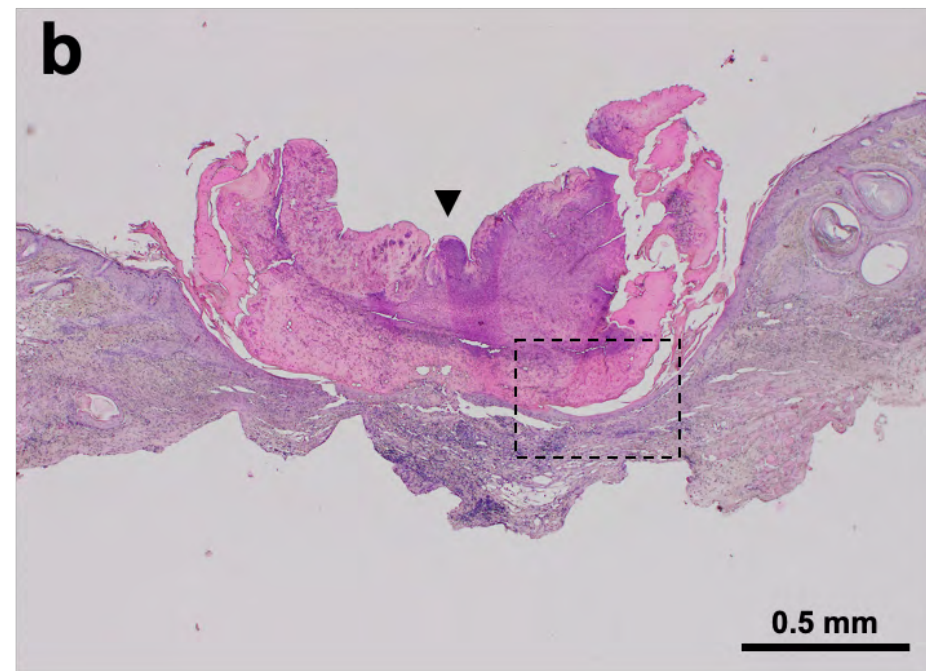
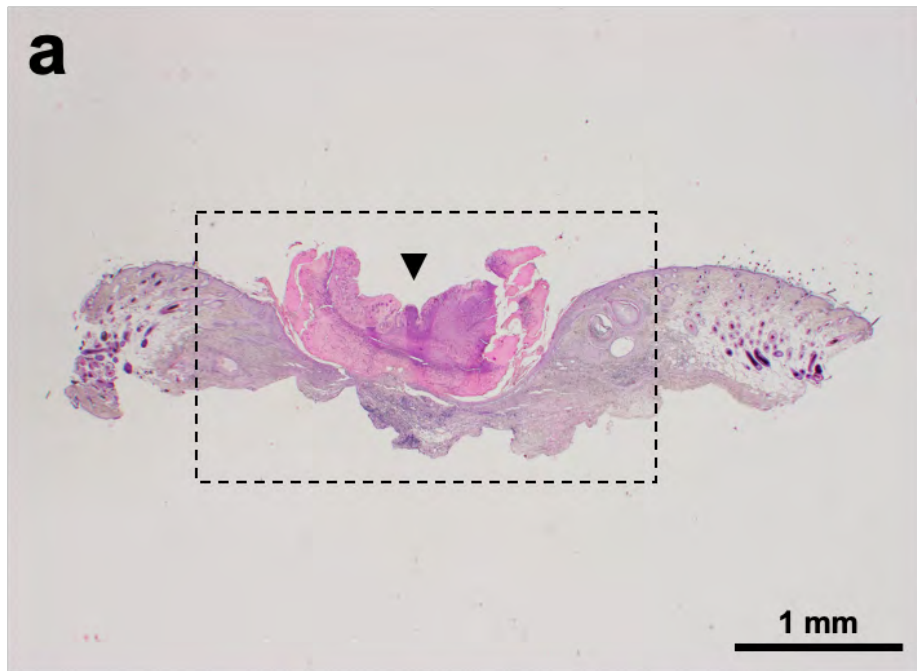


Figure S8. Histopathology 13 days post infection. Panels are (a) 20X, (b) 40X, and (c) 200X. Box in panel a indicates area viewed in panel b. Similarly, the box in panel b indicates field of view of panel c. The wound is significantly smaller than 11 days post infection (Figure S7). Granulation tissue (#, c) and newly formed epidermis (arrow, c) are subjacent to a scab (arrowhead, a-b). Scale bars are as indicated.

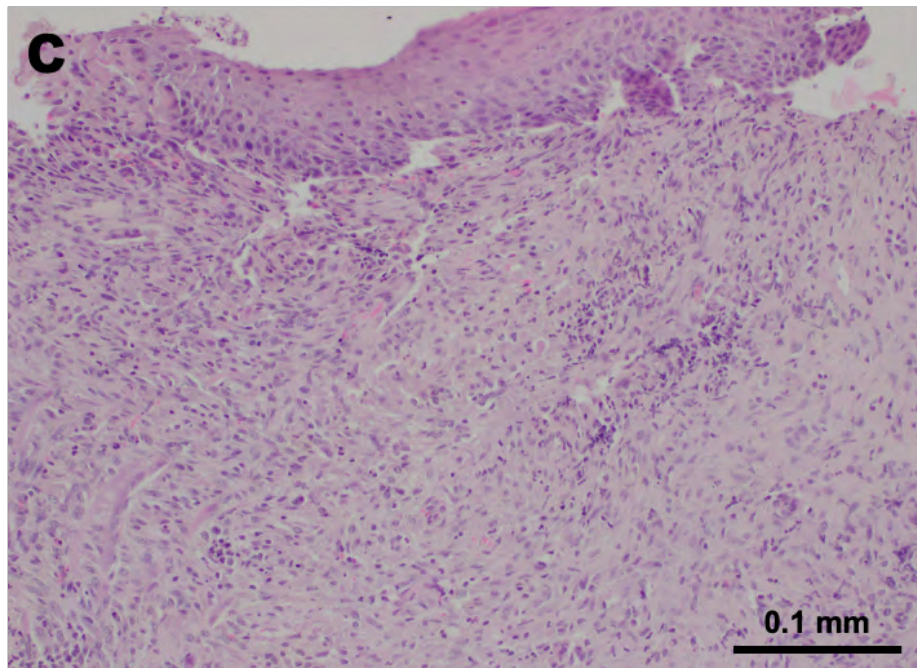
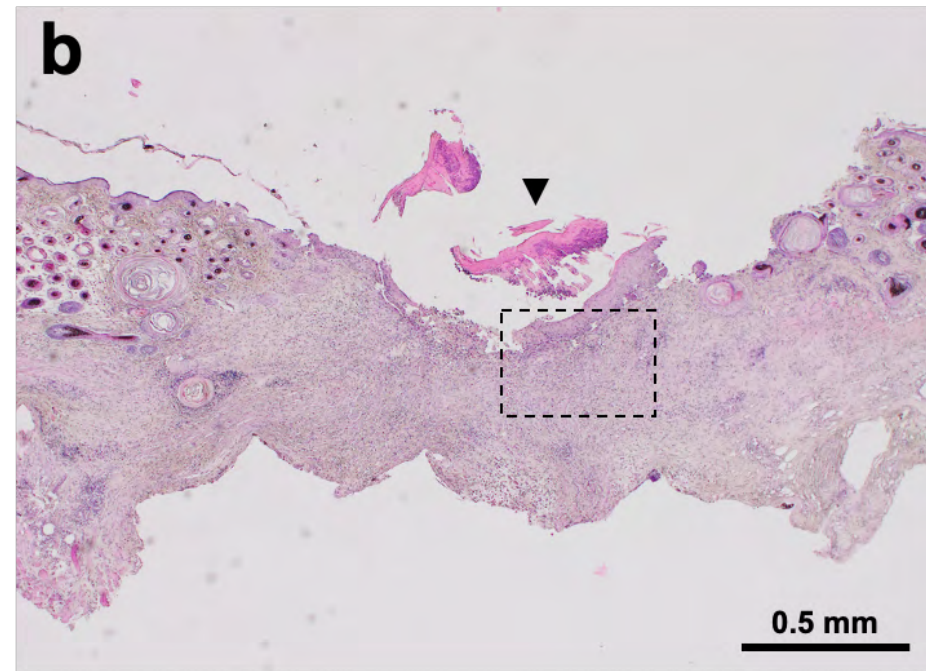
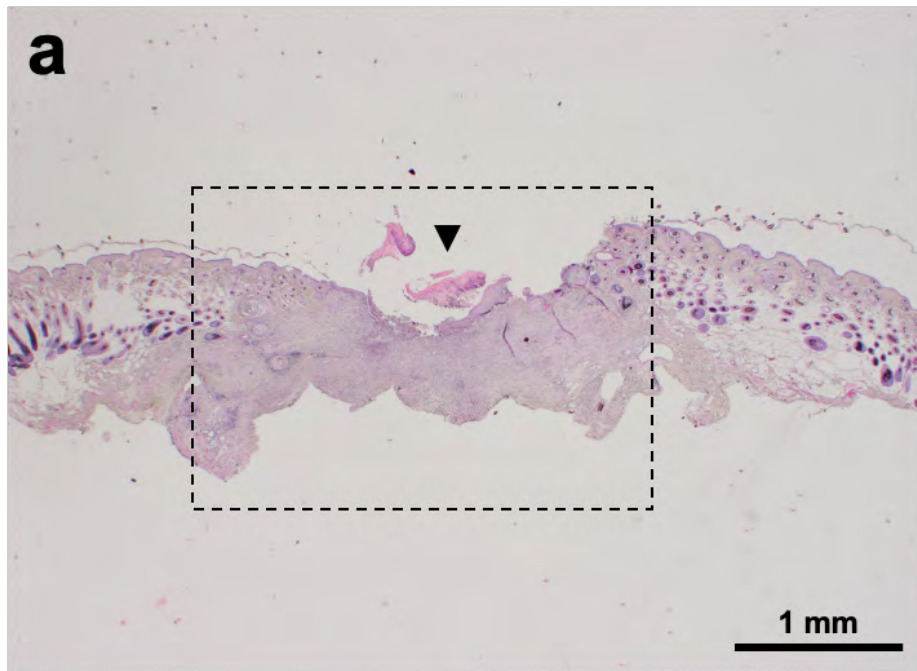


Figure S9. Histopathology 15 days post infection. Panels are (a) 20X, (b) 40X, and (c) 200X. Box in panel a indicates area viewed in panel c. Similarly, the box in panel b indicates field of view of panel c. Reparative changes are predominant. The scab is small and loosely attached (arrowhead, a-b). The wound is almost entirely healed and covered with epidermis. Underneath the newly formed epidermis, there is mature granulation tissue consisting of spindle-shaped fibroblasts, vessels, and sparse inflammatory cells (c). Scale bars are as indicated.

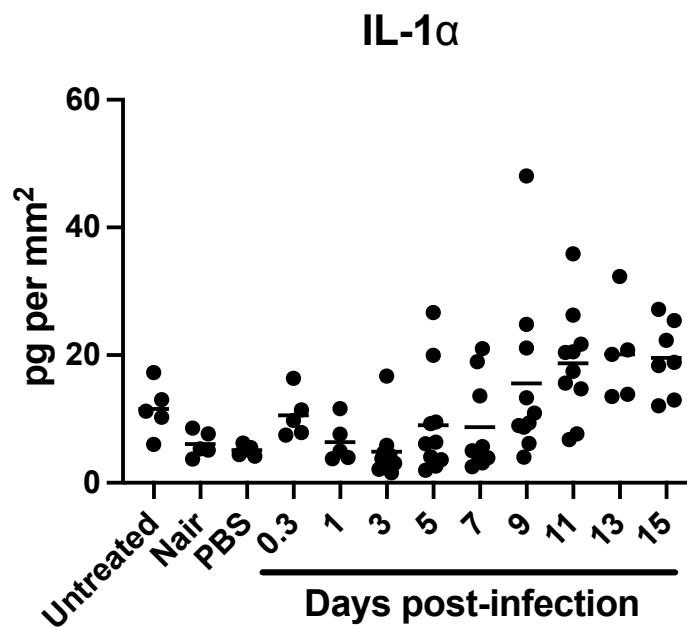


Figure S10. IL-1 α levels in healthy and infected skin. Skin was harvested from untreated mice (i.e. not depilated), control (Nair or PBS), or from infected mice. Pictures were taken after tissue removal to determine the area (mm²) of skin removed. A cytometric bead array assay was performed to quantify IL-1 α level in homogenized skin samples relative to area of tissue removed. Each symbol is an individual mouse and the bars indicates the median (n= 5 – 10 mice/group).

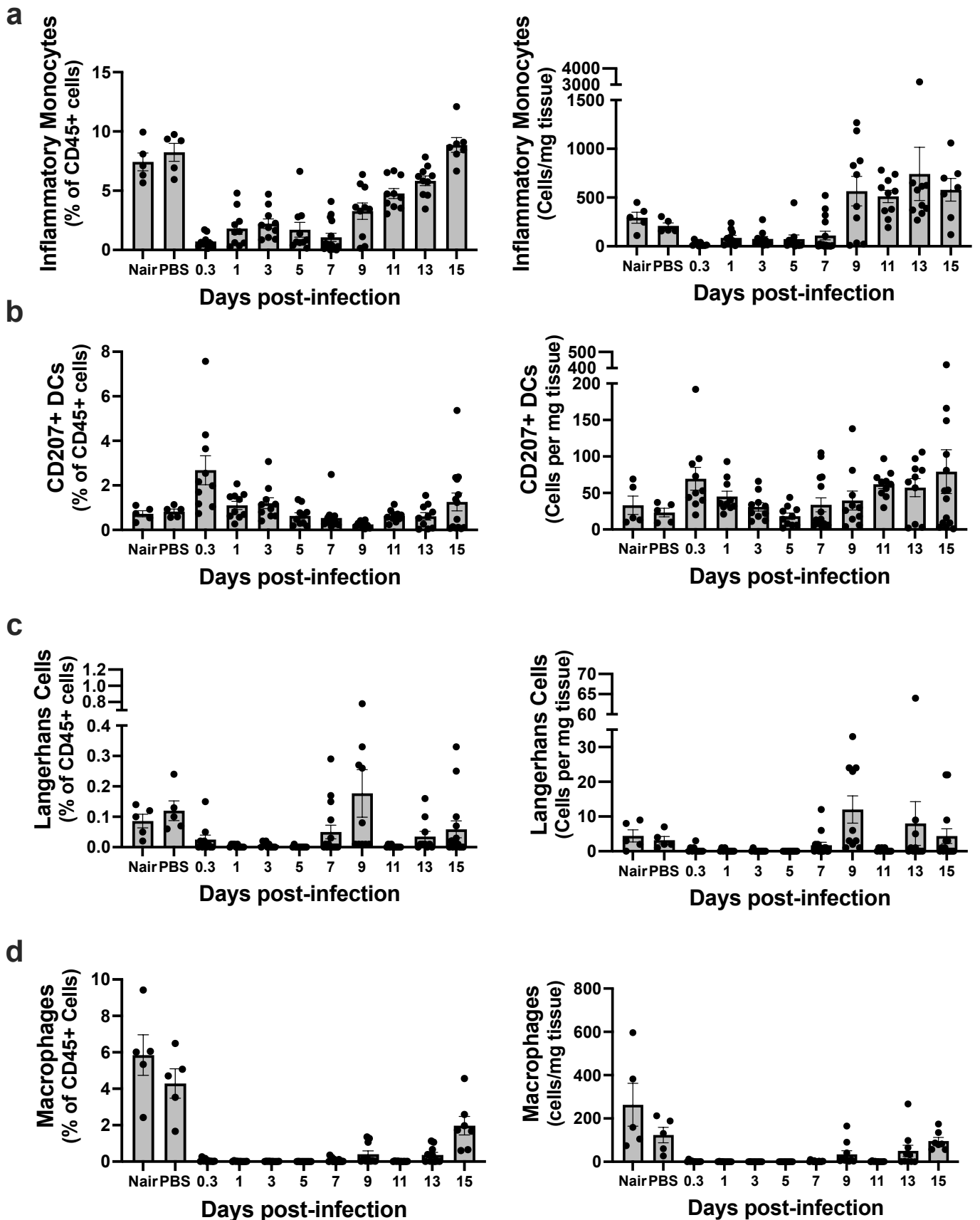


Figure S11: Defined APC populations. Single-cell suspensions derived from skin homogenates from control mice (Nair and PBS) or infected mice isolated at each time point were analyzed to determine the percent and number of (a) inflammatory monocytes (MHCII⁺ Ly6G⁻ CD11c⁻ CD11b⁺ Ly6C⁺ CCR2⁺), (b) CD207⁺ DCs (MHCII⁺ Ly6G⁻ CD11c⁺ CD11b⁻ CD207⁺), (c) Langerhans cells (MHCII⁺ Ly6G⁻ F4/80⁺ CD11b⁺ CD11c⁺ CD207⁺), and (d) F4/80⁺ macrophages (MHCII⁺ Ly6G⁻ F4/80⁺ CD11b⁺). Each symbol represents one mouse. The bars represent the mean and SEM (n= 5-15 mice/group).

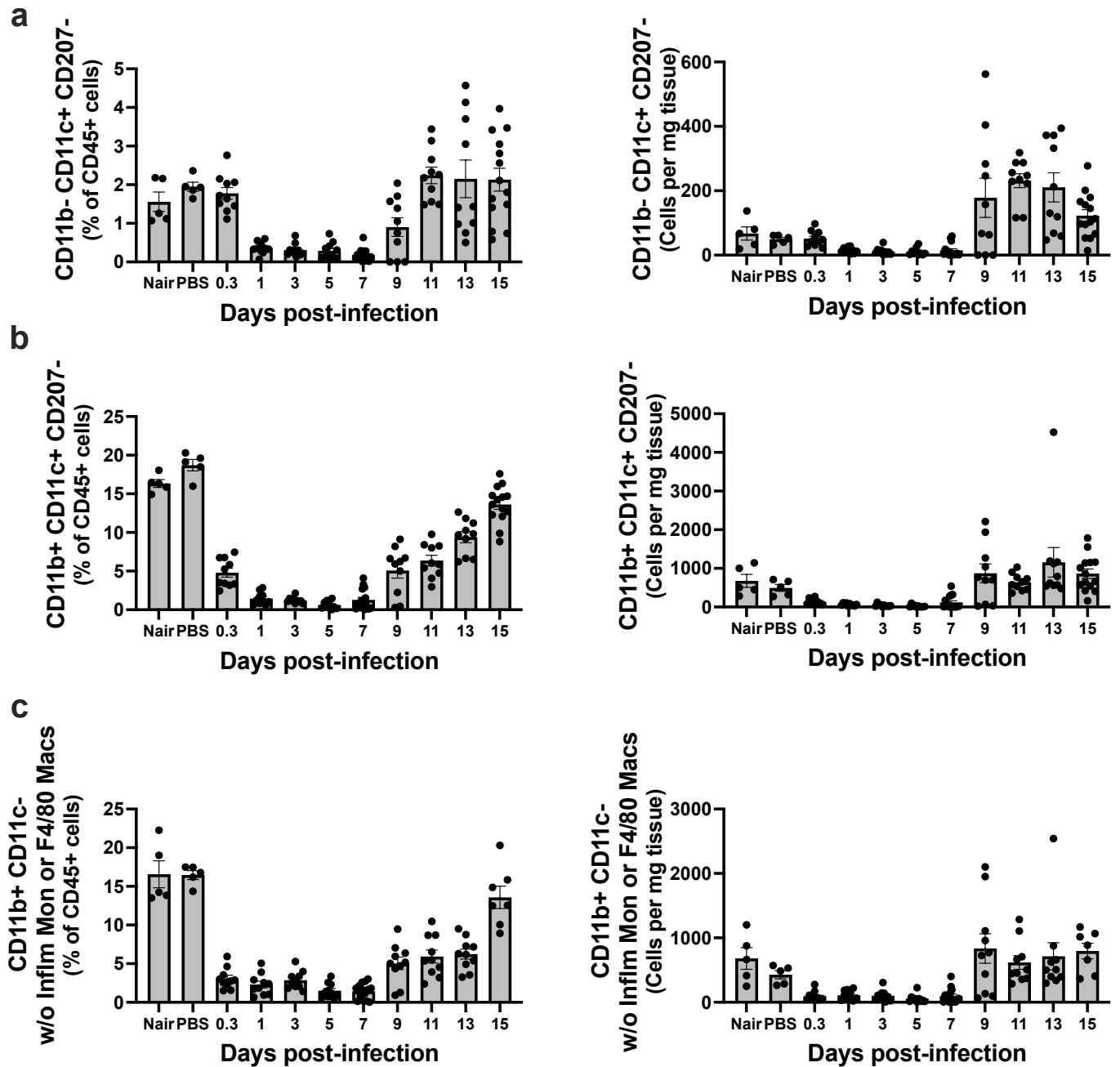


Figure S12: Additional APC populations. Single-cell suspensions derived from skin homogenates from control mice (Nair and PBS) or infected mice isolated at each time point were analyzed to determine the percent and number of (a) MHCII+Ly6G-CD11b-CD11c+CD207-, (b) MHCII+Ly6G-CD11b+CD11c+CD207- that were not inflammatory monocytes or F4/80+ macrophages, and (c) MHCII+Ly6G-CD11b+CD11c- that were not inflammatory monocytes or F4/80+ macrophages. Each symbol represents one mouse. The bars represent the mean and SEM (n= 5 -15 mice/group).

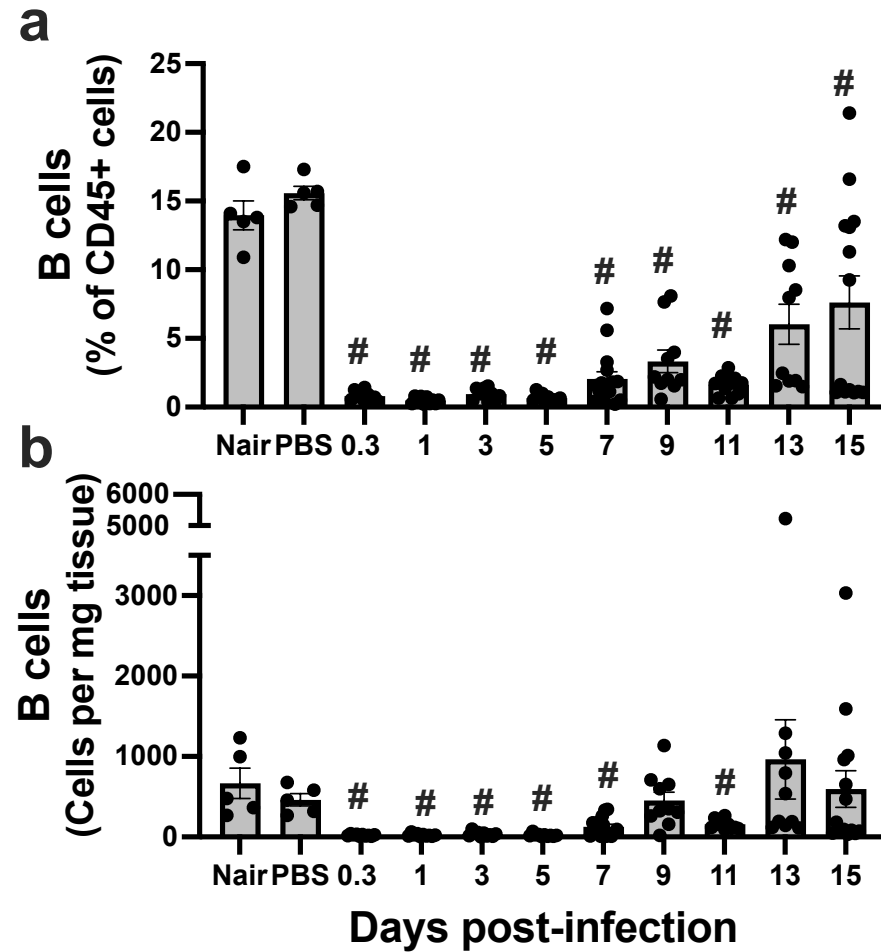


Figure S13. B cell dynamics at the site of infection. Single-cell suspensions derived from skin homogenates from control mice (Nair and PBS) or infected mice isolated at each time point were analyzed to determine the (a) percent or (b) number of B cells (B220+). Each symbol represents one mouse. The bars represent the mean and SEM (n= 5 -15 mice/group).). “#” indicates $p < 0.05$ using Mann-Whitney relative to PBS.

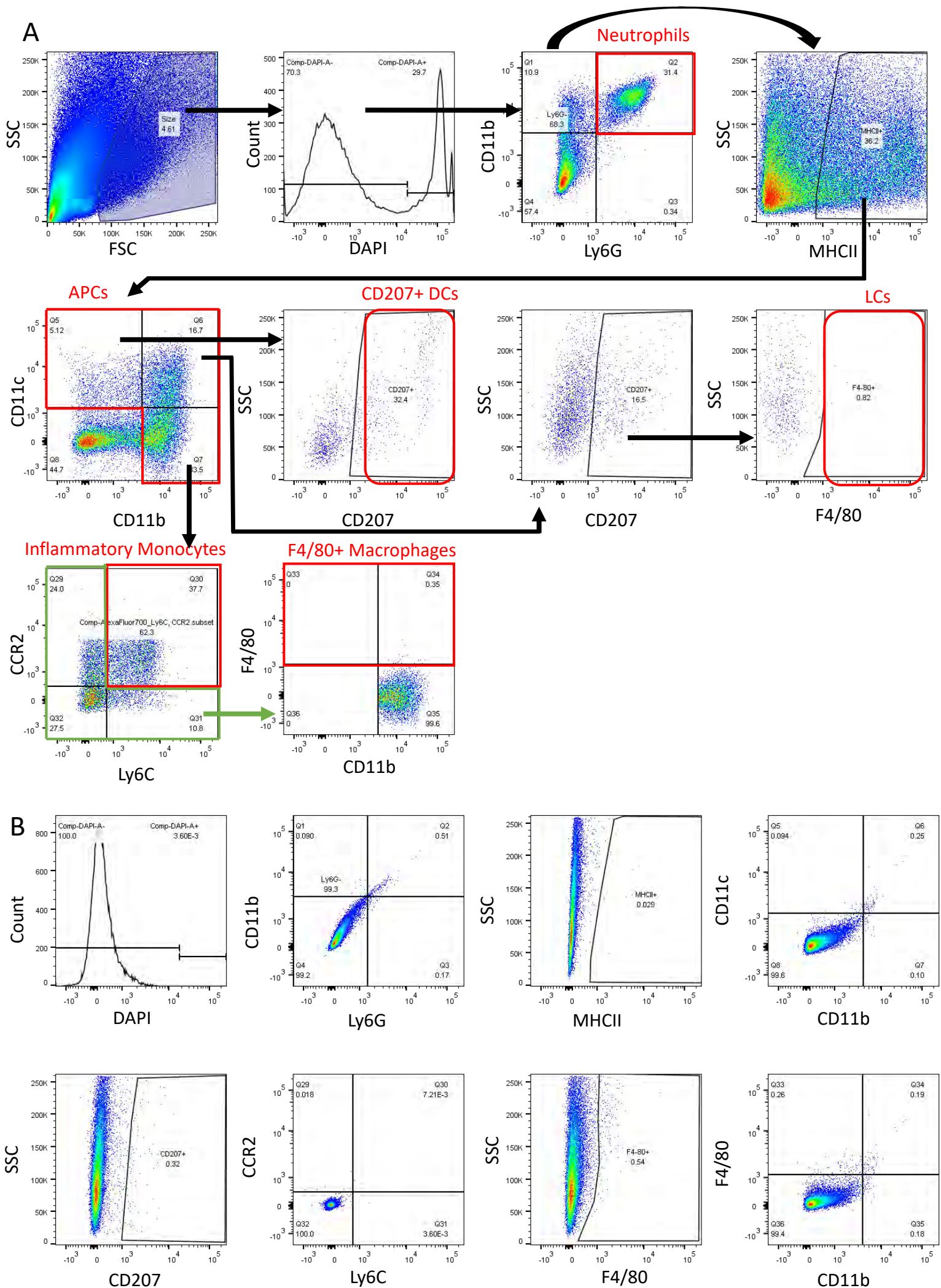


Figure S14. Gating strategy for antibody Panel 1. (A) Representative FACS plots and gating strategy for the APC panel. (B) Unstained controls.

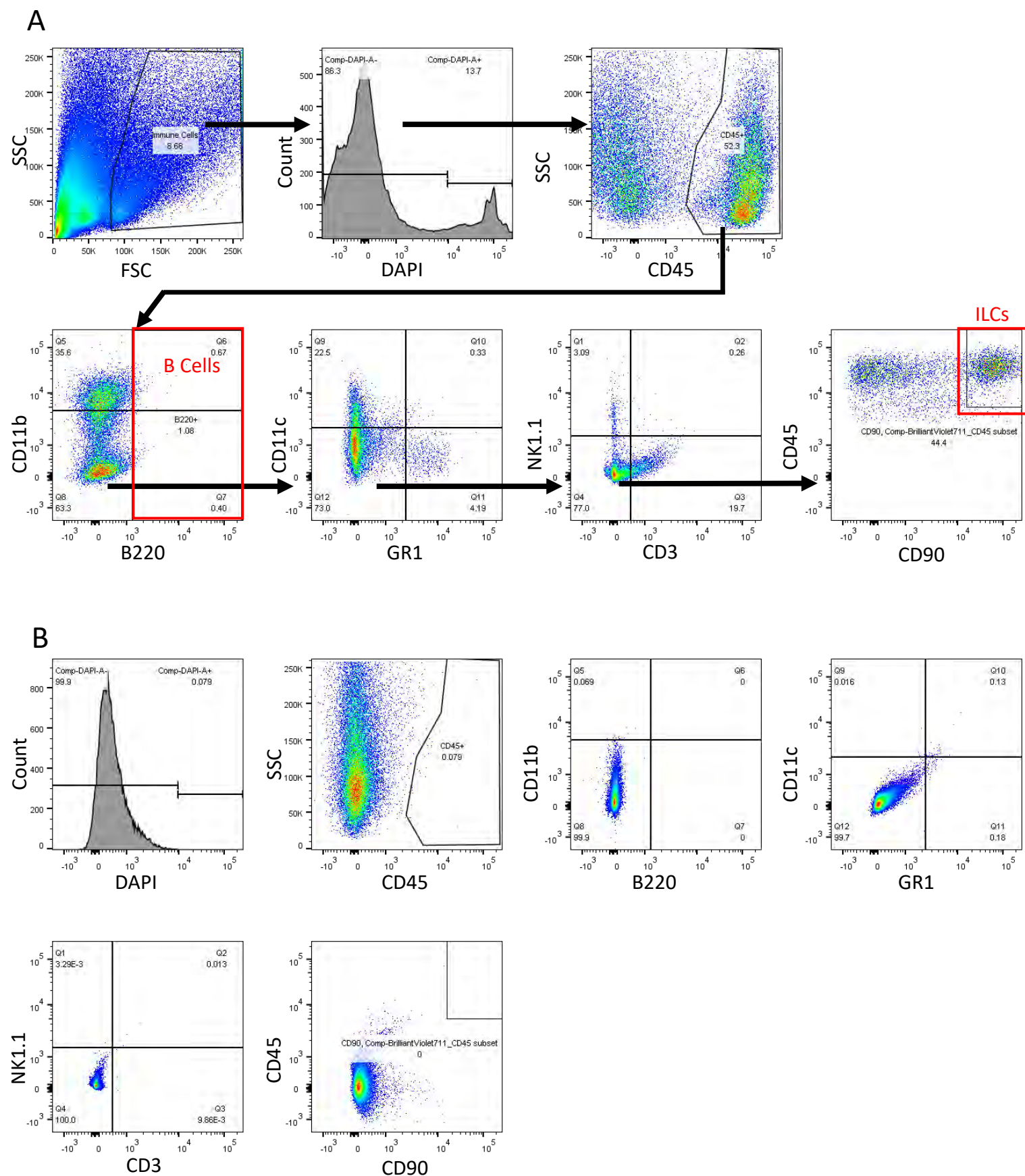


Figure S15. Gating strategy for antibody Panel 2. (A) Representative FACS plots and gating strategy for the ILC panel. (B) Unstained controls.

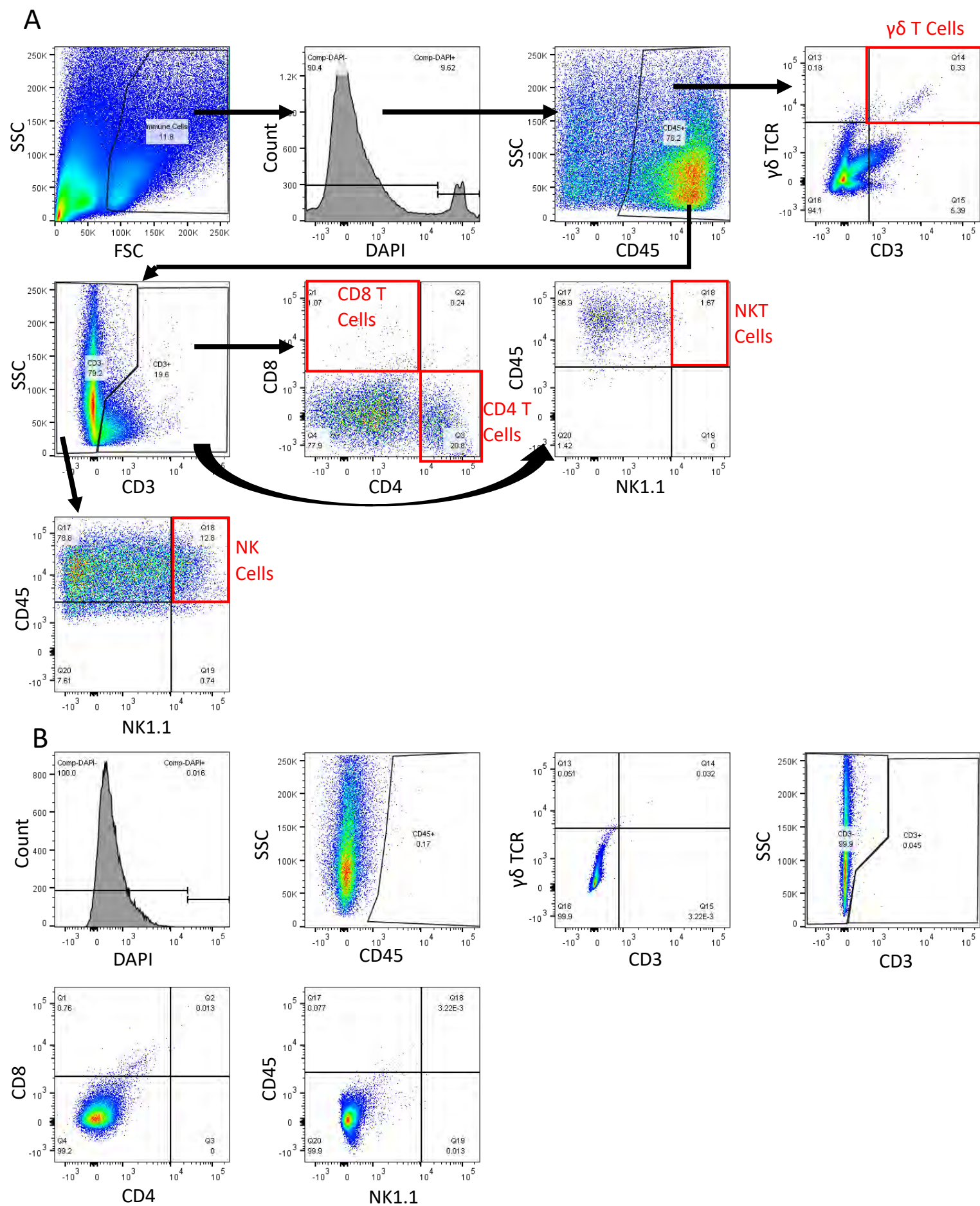


Figure S16. Gating strategy for antibody Panel 3. (A) Representative FACS plots and gating strategy for the T cell panel. (B) Unstained controls.